Evolution towards centrosymmetry of the nonlinear-optical material $RbTiOPO_4$ in the temperature range 293–973 K: Alkaline displacements and titanyl deformations

P. Delarue and C. Lecomte*
Laboratoire de Cristallographie et Modélisation des Matériaux Minéraux et Biologiques, LCM^3B UPRESA 7036, Université Henri Poincaré, Nancy I, Faculté des sciences, Boîte Postale 239, 54506 Vandoeuvre Lès Nancy Cédex, France

M. Jannin, G. Marnier, and B. Menaert
Laboratoire de Physique de l'Université de Bourgogne, LPUB UPRESA 5027, Faculté des sciences Mirande, Boîte Postale 400, 21011 Dijon Cédex, France

(Received 31 October 1997; revised manuscript received 20 March 1998)

The crystal structure of rubidium titanyl phosphate, $RbTiOPO_4$ (space group $Pna2_1$), has been refined at room temperature, and at 473, 673, 873, and 973 K, by using single-crystal x-ray-diffraction techniques. The data show a large anharmonic motion of the rubidium ions increasing with temperature. To describe the importance of this motion in the phase-transition procedure and in the ionic conductivity phenomenon, two models are developed. The study of the deviation to the centrosymmetric structure (space group *Pnan*) shows that the change towards centrosymmetry of the titanyl groups correlates directly with the observed variation of the second-harmonic generating intensity $I_{2\omega}$ of the $RbTiOPO_4$ crystal versus temperature.
[S0163-1829(98)08233-2]

INTRODUCTION

At room temperature and pressure, rubidium titanium oxide phosphate,[1] $RbTiOPO_4$ (RbTP) crystallizes in the acentric $Pna2_1$ space group. In this isotype of $KTiOPO_4$ (KTP), two crystallographically different distorted TiO_6 octahedra are linked through corners, alternately cis and trans, to form unidimensional chains, which are oriented along the *c* optic axis [001].[2] These alternating long and short bond Ti-O chains are bridged by PO_4 tetrahedra forming an open framework containing channels parallel to the *c* axis. The two, not symmetry related, rubidium cations Rb^+, sited in those channels, are relatively free to migrate and contribute to the high anisotropic ionic conductivity (Fig. 1). At high temperature, the KTP family shows a reversible ferroelectric to paraelectric phase transition.[3] The Curie temperature (T_C) of RbTP is in the range 1058–1102 K,[4,5] depending on the crystal growth conditions. After this second-order phase transition, the crystal structure belongs to the centrosymmetric space group: *Pnan*.[6]

Since KTP was introduced as an interesting nonlinear optical material in 1976,[7] many isostructural compounds have received considerable attention. To find correlations[8,9] between the optical nonlinearities [measured as second-harmonic generation (SHG)] and the structural distortions, various definite compounds were studied in different ways. Thomas, Glazer, and Watts[10] deduced, from the comparison of the titanyl (KTP) and the stannyl (KSP) structures, that the Ti-O bonds lengths, which lead to much more distorted octahedra than their SnO_6 counterparts, are elements of correlation. Phillips, Harrison, and Stucky[11] have also compared the potassium, sodium, or silver titanium oxide arsenate, or phosphate, respectively, KTA, KTP, NaTA, NaTP, and AgTP, for which the SHG intensities decrease from 1000 to 0. They find correlations only with the coordination of the mobile cations to oxygen atoms linking the TiO groups and with one of the two angles (Ti-O-Ti). More recently, Allan and Nelmes[12] deduced, from their pressure studies of KTP, that neither the lengths nor the orientations of the Ti-O bonds correlate, at least directly, with the observed variation of SHG power of the crystal versus pressure. As SHG coefficient values are nonzero in a noncentrosymmetric structure, we have studied the evolution of the RbTP structure and its divergence from centrosymmetry versus temperature.

The present work describes the evolution of RbTP lattice parameters, every 50 K from room temperature to 973 K, and of the atomic structure from single-crystal accurate data collected at 293, 473, 673, 873, and 973 K. Besides the anharmonic refinement, another model, which splits the Rb sites, is developed in order to describe their thermal dependence. This structural evolution and its deviation to centrosymmetry are studied in correlation with the evolution of the SHG intensity $I_{2\omega}$ of RbTP.[13,3]

I. EXPERIMENT

A. Data collection and processing

The crystal ($0.24\times0.19\times0.20\ mm^3$) was grown by the flux-growth method.[14] Ag $K\alpha$ x-ray data were collected on an Enraf-Nonius four-circle (CAD4) diffractometer at 293, 473, 673, 873, and 973 ± 3 K. For the high-temperature data collection, we used a locally[15] improved gas-stream heating device,[16] which gives the temperature on the crystal within 3 K. Table I gives some experimental details of the data collection.

The temperature was increased at a rate of 2 K per minute. Every 50 K, this rise was stopped to determine the lattice parameters. The evolution of cell parameters and of the unit-cell volume versus temperature are shown in Fig. 2.

In order to get accurate structure factors, multiple reflections, $(hk\pm1)$ and $(h-k\pm1)$, were collected. During the 80

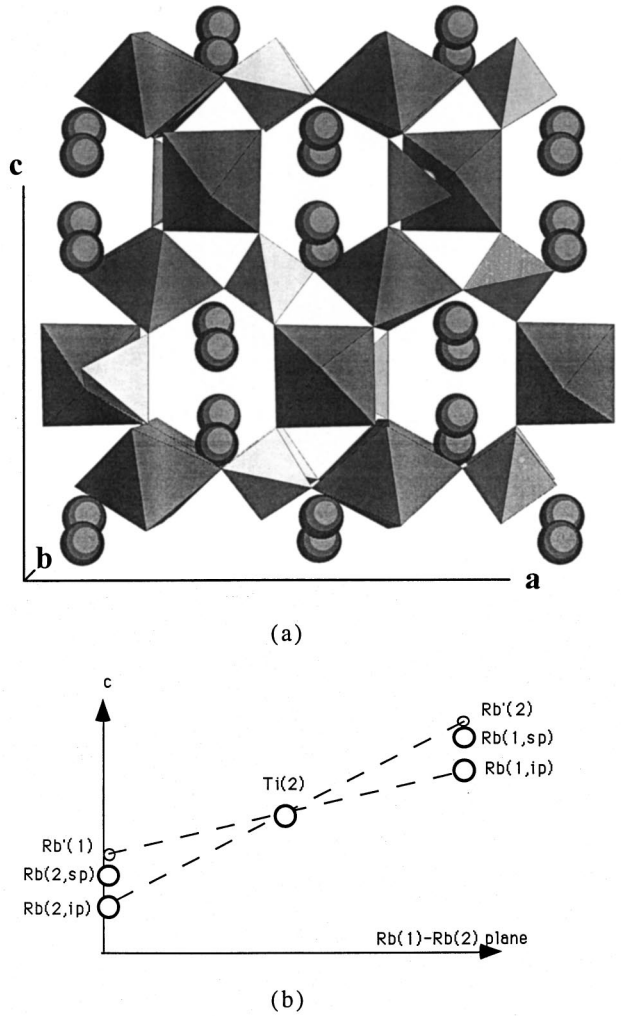

FIG. 1. (a) View of the $RbTiOPO_4$ structure, at 973 K, along the *b* axis. The two pseudoatoms Rb, obtained with the split atom model (sr) in each site, are represented. (b) View of these pseudoatoms positions, at 973 K with Rb′(1) and Rb′(2) as symmetric of Rb(1,ip) and Rb(2,ip) by the (1/4,1/4,1/4) inversion center.

days data collection, the maximum angular deviation in the orientation controls was less than the maximum allowed value (0.08°); owing to the improved sample holder,[15] no reorientation occurred. The standard intensities remained extremely stable during the whole experiment. No measurement above the phase-transition temperature was performed because of the crystal damage: at 1123 K, all intensities fall to few percent after 72 h.

Data reduction and error analysis were performed using the DREAR programs of Blessing.[17] After the background subtraction, the intensities were corrected for the Lorentz and polarization effects. A polynomial fit to the slight decay of the standard reflections intensities (about 3% at 973 K and less than 1% for the other temperatures) over the x-ray exposure time, was applied to scale the data and derive the instrumental instability coefficient ($\langle p\rangle = 1.8\%$) used in the calculation of $\sigma^2(|F|^2) = \sigma_c^2(|F|^2) + (\langle p\rangle |F|^2)^2$.[18] A first absorption correction ($\mu_{calc} = 6.89\ mm^{-1}$) by Gaussian integration method (ABSORB2 program[19]) was made. Then the quality of these corrected intensities was improved by the Blessing empirical absorption method (SORTAV[20]): a spherical harmonic expansion in real form up to $l=6$ for even order and $l=3$ for odd order was found optimal to fit the absorption anisotropy. This procedure using these two absorption corrections improved the consistency of the data (decrease of the internal agreement factor R_{int}, Table I).

B. Least-squares refinements

At room temperature, xyz and anisotropic harmonic thermal displacement U^{ij} parameters of KTP (Ref. 21) were used as starting parameters for the 293 K refinement [MOLLY (Ref. 22)]; to refine the structure at the other temperatures, the parameters of nearest temperature were used as a starting point. In all cases, the Rb atoms were refined as ions (Rb^+ scattering factors[23]); the residual charge was distributed on the ten oxygen atoms. The core and radial valence scattering factors for non-Rb atoms were calculated from Clementi wave functions.[24] The anomalous dispersion of each atom[25] was taken into account. To obtain the thermal displacement parameters of the Rb ions, three strategies have been used.

Harmonic model (hm): after refinement of the *x*, *y*, *z*, and U^{ij} parameters against the room-temperature data (Table I), the agreement indices *R*, R^w, *Z* are excellent. At higher temperatures, the anisotropic refinements did not converge well: they led to nonpositive definite thermal ellipsoids for some oxygen atoms, and the residual density $\Delta^{res}\rho(\mathbf{r})$ in the Rb regions increased a lot with temperature.

Anharmonic model (am): therefore the harmonic $T_0(\mathbf{H})$ Debye-Waller factor was corrected by the Gram-Charlier series expansion which is a Taylor-series-like expansion using the rectilinear Gaussian probability density functions and its successive derivatives.[26] As programmed in MOLLY,[22] the thermal anharmonic $T(\mathbf{H})$ becomes

$$T(\mathbf{H}) = T_0(\mathbf{H})\left[1 + \frac{i^3}{3!} C^{jkl} h_j h_k h_l + \frac{i^4}{4!} D^{jklm} h_j h_k h_l h_m + \cdots\right]$$

(where C^{jkl} and D^{jklm} are the third- and the fourth-order Gram-Charlier coefficients, respectively).

To reduce the number of parameters to the minimum, only Rb atoms were anharmonically refined up to the fourth-order Gram-Charlier coefficients. In spite of high correlation coefficients (>0.80) between the fourth- and the second-order [$T_0(\mathbf{H})$], amplitudes of some anharmonic coefficients are significant; their values increased with temperature (mainly: $C^{333}, C^{233}, D^{3333}, D^{2333}\ldots$ see supplementary material[27]). This model improved the fit significantly (Table I).

Figure 3 gives the evolution of the thermal displacement parameters. The average value of U_{eq} [$U_{eq} = (U^{11} + U^{22} + U^{33})/3$] for each type of atom is linear versus temperature. For Ti, P, O, this straight line passes through the origin [Fig. 3(a)], but this is not the case for Rb. The evolution of the U^{ij} ellipsoid thermal coefficients of Rb(1) and Rb(2) are similar [Fig. 3(b)]. Only the U^{33} straight line does not intercept the origin. At 0 K, its value is negative, which is physically wrong in the harmonic approximation. Despite a refinement at the fourth order of the Gram-Charlier coefficients for the Rb, modeling each Rb ion by a single site is not adequate. It

TABLE I. Details of data collections and refinements.

Temperature (K)	293	473	673	873	973
Lattice parameters (Å) a	12.952(1)	12.978(1)	13.013(1)	13.051(1)	13.071(1)
b	6.4925(5)	6.5109(5)	6.5339(5)	6.559(1)	6.575(1)
c	10.555(1)	10.542(1)	10.519(1)	10.494(1)	10.478(1)
$[\sin(\theta)/\lambda]_{max}$	1.29	1.29	1.16	1.08	1.13
No. of reflections measured	10667	12732	10908	10093	9225
No. of refl. used for refin. $I>3\sigma$	4397	5053	3694	2895	2733
$R_{int.}$[a] (%)	2.03	2.22	2.53	2.5	2.3
Refinement program	MOLLY (Ref. 22)				
Model hm					
Number of parameters	145				
Scale factor	0.1852(3)	0.1862(3)	0.1790(4)	0.1836(9)	0.1863(7)
R[b] (R_w[c]) (%)	2.87(3.64)	4.06(4.27)	5.12(6.11)	6.77(8.9)	6.85(7.76)
Goodness of fit Z[d]	1.68	1.84	2.5	4.31	3.51
Model am					
Number of parameters	195				
Scale factor	0.1877(3)	0.1894(3)	0.1880(3)	0.1869(4)	0.1863(3)
R[b] (R_w[c]) (%)	2.61(3.34)	3.22(3.23)	2.93(3.16)	2.86(3.17)	2.83(2.63)
Goodness of fit Z[d]	1.55	1.4	1.31	1.55	1.21
Extinction parameters[e]	1.99(7)	3.30(8)	3.6(1)	2.8(1)	1.41(6)
Model sr					
Number of parameters	165				
Scale factor		0.1888(3)	0.1882(3)	0.1873(4)	0.1864(3)
R[b] (R_w[c]) (%)		3.25(3.27)	2.95(3.21)	2.94(3.16)	3.03(2.73)
Goodness of fit Z[d]		1.41	1.32	1.54	1.24
Extinction parameters[e]		3.25(8)	3.5(1)	2.7(1)	1.41(6)

[a] $R_{int}=(\Sigma|Y-Y_{mean}|)/\Sigma|Y|$, average of equivalent reflections in mm^2 symmetry [SORTAV (Ref. 20)].
[b] $R=[\Sigma(|F_o|-|F_c|)/\Sigma|F_o|]$, where F_o and F_c are the observed and calculated factors respectively, w is the weight assigned to each reflection, N is the number of independent reflections, and n is the number of refined parameters.
[c] $R_w=\{\Sigma[w(|F_o|-|F_c|)^2]/\Sigma w|F_o|^2\}^{1/2}$, see footnote b.
[d] $Z=\{\Sigma[w(|F_o|-|F_c|)^2]/(N-n)\}^{1/2}$, see footnote b.
[e] Isotropic extinction, type 2, Lorentzian and Nelmes-Thornley mosaic distribution.

needs a model which splits the Rb ions on two sites elongated along the c axis. The distance between these two atoms must decrease to zero at 0 K.

Splitting of the Rb sites model (sr): the anharmonic approximation (am) has been replaced by splitting each Rb atom onto two independent sites. The sum of the multiplicity of these two sets of pseudoatoms was constrained to be 1 during all refinements. At 293 K, the short distance between the two pseudo-Rb ions in each Rb(1) and Rb(2) site, leads to a much too strong correlation between their x, y, z, U^{ij}, and occupancy parameters. Therefore, at room temperature, we used the harmonic model (hm). At 473 K, x, y, z, and U^{ij} calculated from am, were used as starting parameters. For each Rb ion, two pseudoatoms labeled with subscripts ip and sp, were originally located at the x_{Rb},y_{Rb},z_{Rb} sites with multiplicity of 0.9 and 0.1, respectively. During the refinement process these two atoms split naturally towards different positions. At the end of the refinement, at $T=473$ K, the distances between the two pseudoatom sites were 0.27(1) and 0.19(1) Å along the c axis for Rb(1) and Rb(2), respectively. Then, the results of each refinement were used for the refinement of the structure at the next temperature. Despite some correlation (>0.85) between the Rb pseudoatom parameters due to these short distances (maximum 0.8 Å for 973 K), this model improved the fit significantly for all temperatures studied.

Furthermore, at 973 K, for all models, we observed systematically high correlation coefficients $[0.73<\mathrm{corr}(i,j)<0.95]$ between the temperature factors and the position parameters of all oxygen and rubidium atoms which are related by the inversion center in the high-temperature centrosymmetric phase. Positional and thermal parameters obtained for hm, am, and sr models are given in supplementary material. All the structure parameters remain the same within estimated errors except for Rb.

II. RESULTS AND DISCUSSION

A. Lattice parameters

Figure 2 shows the evolution of the volume and of the lattice parameters versus temperature. If the volume, and the a and b parameters increase with the temperature, c decreases. As expected, the evolution of lattice parameters is similar to that observed, at room temperature, by Zumsteg, Bierlein, and Gier[7] in the study of $K_{1-x}Rb_xTP$ solid solution: a and b increase by 1.2 and 1.6 %, and c decreases by 0.3% when x goes from 0 to 1. In our case, temperature has the same effect as the Rb concentration in the solid solution. Our measurements of the lattice parameters allow the calculation of the thermal-expansion coefficients (Table II). Our values are higher in magnitude that those given by Chu, Bierlein,

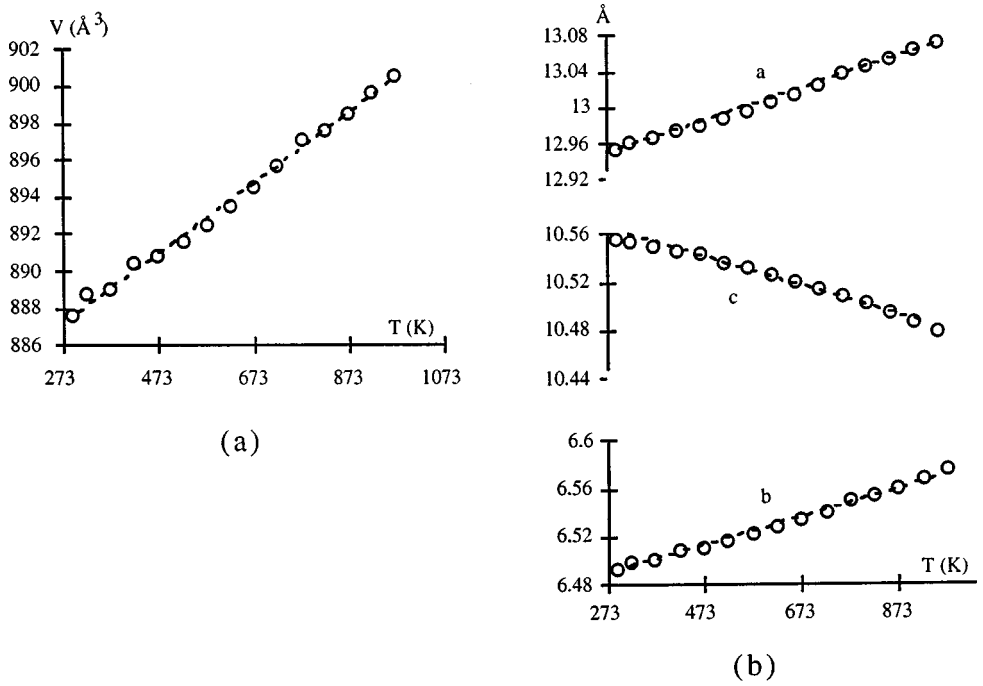

FIG. 2. Evolution of the volume ($Å^3$) (a) and of the parameters a,b,c (Å) (b) of the cell versus temperature (K).

and Hunsperger[28] obtained from dilatometer measurements. These discrepancies can be explained by differences in crystal purity and also by considering our results are averaged over 293–973 K (680 K), i.e., a much larger than for the dilatometer data [293–373 K (80 K)].

At 1193 K, all x-ray intensities vanish. For example, the intensity of the reflection $(0\ 2\ \overline{10})$ decreases by more than 70% in 46 h. The decrease of *a* and *b*, and the increase of *c* lattice parameters (see in supplementary material[27]), during that time, is in favor of a loss of Rb.

B. Validity of the splitting Rb sites (*sr* model)

The residual density maps (not given in this paper) calculated from the harmonic model (*hm*), show two residual positive peaks around the Rb sites along the *c* axis. Then in the *sr* model, each Rb site has been split into two independent pseudoatoms, Rb(1,*ip*), Rb(1,*sp*) for site 1, Rb(2,*ip*) and Rb(2,*sp*) for site 2, corresponding, respectively, to the initial room temperature position, *ip*, and to the high-temperature split position, *sp*. The *sr* model describes more precisely the evolution of the Rb ions. This is confirmed by the linear evolution of the rubidium equivalent thermal dis-

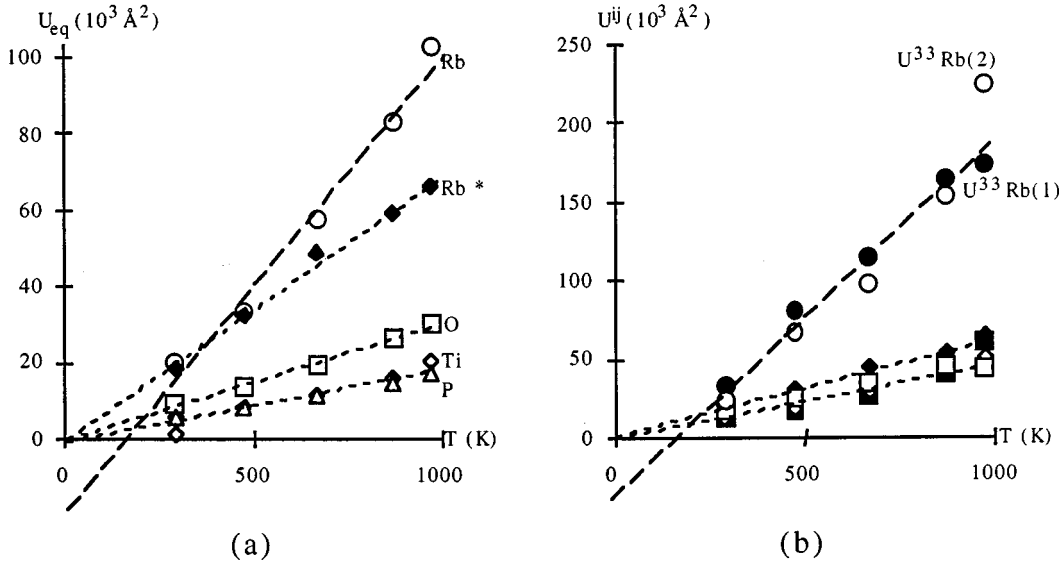

FIG. 3. Evolution of the average value of U_{eq} thermal motion (*am* model) for each type of atom (10^3 Å^2) (a) and evolution of U^{ii} for each Rb(1) and Rb(2) site (10^3 Å^2) (b), versus temperature (K). The asterisk indicates an average value of U_{eq} for Rb atoms with the split atom model (*sr*).

TABLE II. Thermal-expansion coefficients (ppm/K).

	Our work	Correlation coefficient	Dilatometer data (Ref. 28).
α_{11}	13.5(6)	0.997	10.8
α_{22}	18.4(6)	0.997	13.3
α_{33}	−10.5(3)	0.992	−5.9

placement parameters U_{eq}, for which the temperature plot passes through origin [Fig. 3(a)]. Moreover, qualitatively, the evolution of the heights and of the distance between the two peaks on the *hm* residual density maps, which increase with the temperature (Table III), is in a good agreement with the positions of the Rb(*sp*) and Rb(*ip*) pseudoatoms obtained from the *sr* model. As harmonic refinement of a single atom shifts the position of Rb towards the center of mass of both Rb(*sp*) and Rb(*ip*) pseudoatoms, and is not able to take into account the electron density which is far away, these positions and heights of the residual peaks, quantitatively, do not match exactly with the results derived for the split Rb model.

C. Thermal displacement of Rb ions

Figure 4 gives the thermal dependence of each Rb displacement calculated from *am* and *sr* models. In the anharmonic model (*am*), the displacements of the Rb ions from their room-temperature positions, are small in the *a* and *b* directions contrary to the *c* direction [Figs. 4(a) and 4(b)]. In this hypothesis, the *am* Rb positions are the weighted mean values of the two pseudo-Rb positions obtained from the *sr*. So, in the split atom model, the displacements and the distances between the two pseudo-Rb ions are negligible in the *a* and *b* directions within experimental errors. Therefore the major effect of temperature is the displacement of the Rb ions along the *c* axis.

Along the *c* axis, in the anharmonic approximation, the Rb ion positions change gradually with temperature. At 973 K, the Rb ions move about 0.5 Å away from their room-temperature positions. At this temperature, both Rb(1) and Rb(2) ions are almost related by an inversion center at (1/4,1/4,1/4) within 0.1 Å. On the other hand [Figs. 4(c) and 4(d)], the split atom model (*sr*) shows that the initial room-temperature position, *ip* of each Rb ion does not change, only *sp* moves; it also demonstrates that the occupancy of the *ip* sites decreases when the temperature increases. Therefore, from 473 K, the occupancies of the split *sp* sites increase and their positions move gradually away from the initial room-temperature positions *ip*. At 973 K, the occupancies are about 60% for displacements of 0.8 Å.

At room temperature, the Rb atoms occupy large cavities enclosed by the oxygen framework. Rb(1) is coordinated by eight oxygen atoms giving rise to four short bonds [2.74<Rb(1)-O<2.84 Å], and four long interactions up to 3.23 Å. Rb(2) shows a nine oxygen atoms coordination, with three short bonds [2.74<Rb(2)-O<2.86 Å], and six others up to 3.13 Å. At 973 K, the split atom model (*sr*) shows that the distances Rb(1,*ip*)-Rb(2,*sp*) and Rb(2,*ip*)-Rb(1,*sp*) are about 3.51 and 3.21 Å. Numbering dummy atoms Rb′(1) and Rb′(2) as the symmetric of Rb(1,*ip*) and Rb(2,*ip*) by the (1/4,1/4,1/4) inversion center [Fig. 1(b)], the distances Rb(1,*ip*)-Rb′(1) and Rb(2,*ip*)-Rb′(2) are about 3.3 and 3.0 Å. Then, at 973 K, the pseudoatoms *sp* are near Rb′(1) and Rb′(2) positions. On the other hand, in KTP, at room temperature, Thomas and Glazer[29] show that the domain twinning is due to the displacements of the K ions onto their respective hole sites [corresponding to Rb′(1) and Rb′(2)] which are related by pseudosymmetry to the inequivalent potassium sites K(1) and K(2). They deduce that the ionic diffusion paths for K^+ along [0 0 1] involve both potassiums and hole sites. Our work confirm that the diffusion paths in the ionic conductivity phenomenon is Rb(1,*ip*)-Rb′(2)-Rb(2,*ip*)-Rb′(1). Moreover, if the high-temperature (up to 1073 K) positions of Rb ions lie halfway between the initial room-temperature *ip* position and their associated Rb′ sites, it could explain the loss of Rb, by thermal motion inducing self-ionic-conductivity.

D. Divergence of centrosymmetric structure and SHG properties

To calculate the deviation from centrosymmetry, we use the MISSYM program[30] which determines the minimum average deviation of the atoms (the ''tolerance'') to find ''unseen pseudosymmetry'' relationships. In all cases, whatever the temperature and the model used, MISSYM has detected an inversion center at (1/4,1/4,1/4) and a [001] perpendicular *n*-glide plane (*x y* 0), corresponding to the *Pnan* space group, as observed for the paraelectric phase of TITP.[6] When the atoms of the TiO_6/PO_4 framework are investigated separately from all the structure, i.e., without the Rb ions [Figs. 5(a) and 5(b)], the deviations calculated are much smaller than those given by all the structures. Then, these largest deviations are only due to the Rb ions.

With the parameters obtained by the anharmonic refinement (*am*), the deviation of Rb ions from *Pnan* symmetry

TABLE III. Residual density peaks (*hm* model) and distance between the two pseudo-Rb ions (*sr* model).

Temperature (K)	Distance[a] between the two peaks (Å)		Heights of the two peaks for each Rb site (eÅ^{-3})				Distance[a] between the 2 atoms (Å) (model *sr*)	
	Rb(1)	Rb(2)	Rb(1)		Rb(2)		Rb(1,*ip*,-*sp*)	Rb(2,*is*-*sp*)
293	0.62	0.44	1.5	2	1	1		
473	0.75	0.62	2.5	3	1	2	0.27	0.19
673	1.06	1.06	2.5	3.5	1	3	0.48	0.38
873	1.06	1.06	3	3	3	3.5	0.66	0.56
973	1.06	1.06	2.5	2.5	3	3	0.77	0.68

[a]Distance along the *c* axis.

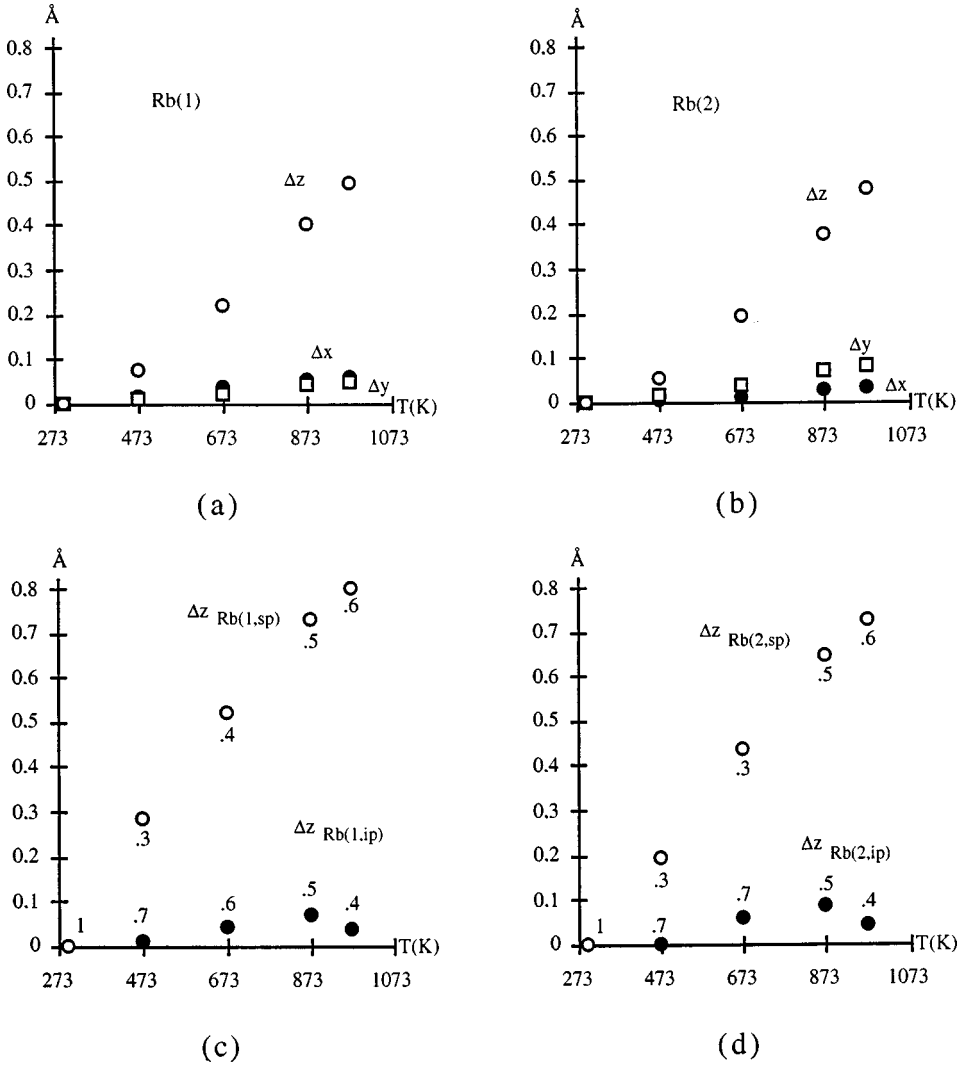

FIG. 4. Evolution of the displacements (Å) of each Rb(1) (a) and Rb(2) (b) ion along the *a*, *b*, and *c* axes, from the room temperature, versus temperature *T* (K) ($\Delta X = X_T - X_{293\,K}$ where $X = x$, *y*, or *z*), and evolution of the displacements (Å) along the *c* axis, from the initial room-temperature position *ip*, of *ip* and *sp* pseudoatoms with their associated multiplicity for each Rb(1) (c) and Rb(2) (d) site versus temperature *T* (K) ($\Delta z = z_{p,T} - z_{ip,293\,K}$ where $p = ip$ or *sp*).

decrease gradually from 0.53 Å at room temperature to 0.08 Å at 973 K [Fig. 5(a)]. This evolution corresponds to a convergence of the Rb ion positions toward centrosymmetry. But when the Rb ions are split (*sr* model), the Rb (*ip*) tolerance remains quite constant with temperature. On the other hand, the Rb (*sp*) deviation value begins to decrease from 0.53 Å at room temperature to 0.05 Å at 673 K and then increases to 0.24 Å at 973 K [Fig. 5(b)]. Consequently, the split atom model shows that the Rb ions reach ''unstable'' centrosymmetry, in this structure.

Within the framework only, the calculated deviation (about 0.18 Å at room temperature) is three times smaller than that calculated with the whole structure, but it starts to decrease only at 873 K [Figs. 5(a) and 5(b)]. At 973 K, this deviation is reduced by half. At temperatures higher than 1073 K (phase-transition temperature), the crystal structure should be in space group *Pnan*, so the tolerance must be zero. This evolution corresponds exactly to the evolution of the second-harmonic-generating (SHG) intensity $I_{2\omega}$ of RbTP versus temperature[3] [Fig. 5(d)]. On the other hand, at 873 K, the occupancies of the initial Rb ion positions *ip* are reduced about 50%. Then, the displacements of the Rb ions seems to be the principal feature of the structural phase transition which is a second-order transition.[3] Hence, it is accompanied by large displacements (more than 0.5 Å, parallel to the *c* axis) of Rb ions from their room-temperature position.[31]

The displacement of the P atom from the geometric center of its four oxygen atom neighbors Δ_{tet} is negligible ($\Delta_{tet} = 0.03$ Å at room temperature) compared to the evolution of the octahedral distortions Δ_{oct} (displacement of the Ti atom from the geometric center of its six oxygen atom neighbors). So, the evolution of the framework expresses mainly in the evolution of the octahedral distortions. Δ_{oct} [Ti(1)] remains approximately unchanged [about 0.21(1) Å] up to 673 K and decreases to about 0.16(1) Å at 973 K. Δ_{oct} [Ti(2)] remains also approximately unchanged [about 0.15(1) Å] up to 673 K, then it falls quickly to about 0.05(1) Å at 973 K [Fig. 5(c)]. Another measurement of the octahedral distortion[10] is to find the mean *M*-O bond lengths and then to calculate the average deviations from the means [i.e., $(\Sigma_i^6 |(x_i - \overline{x})|/6)$]. In this case, the average deviations from the means for Ti(1) is

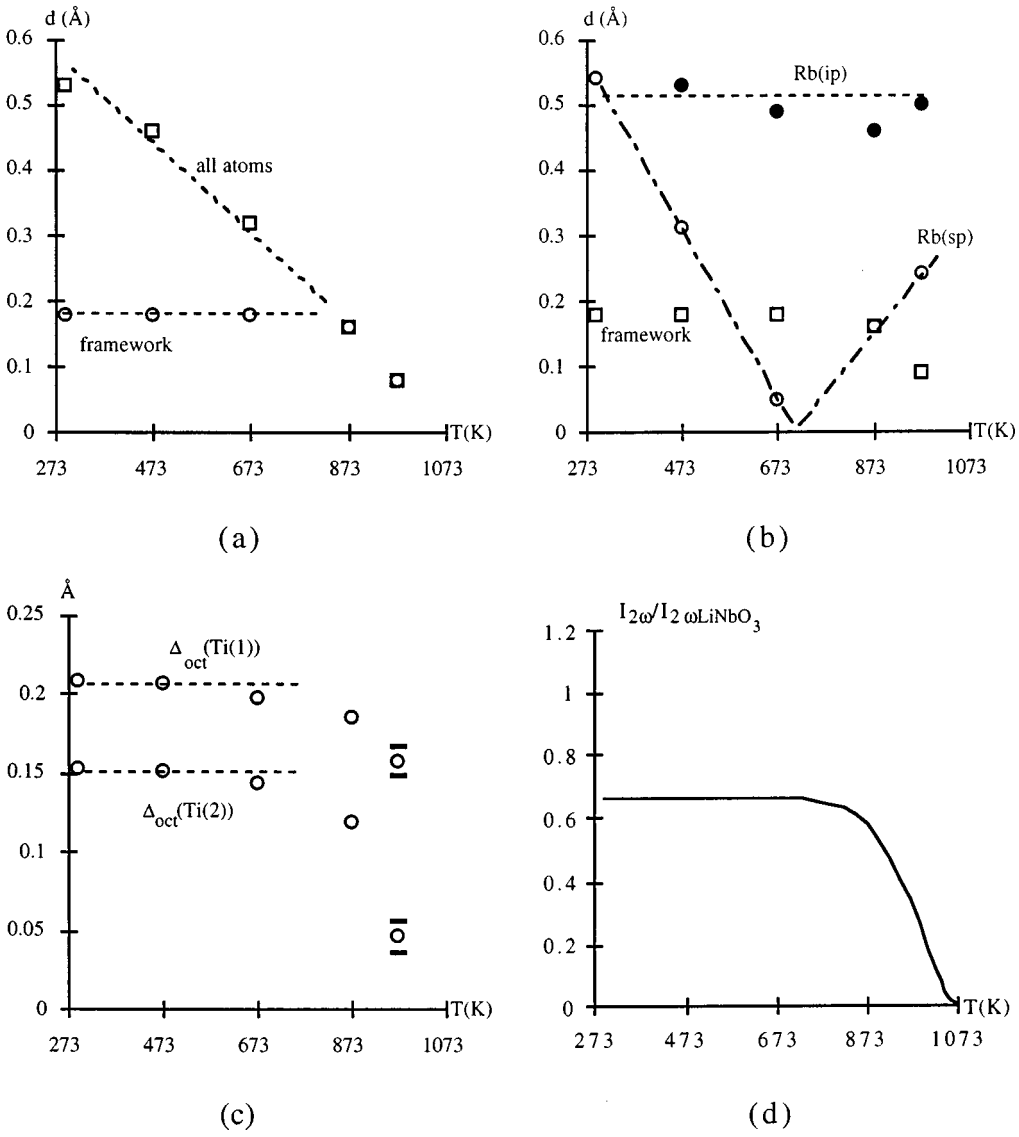

FIG. 5. Program MISSYM (Ref. 30): evolution of the distance (Å) to the average position of pseudosymmetry plane or inversion center considering all crystal structure or only the TiO_6/PO_4 framework, versus temperature (K) (a) anharmonic model (am), (b) split atom model (sr). (c) evolution of the octahedral distortions Δ_{oct} (displacement of the Ti atom from the geometric center of its six oxygen atom neighbors) for the Ti(1) and Ti(2) sites, versus temperature (K). (d) temperature (K) dependence of SHG intensity $I_{2\omega}$ (Fig. 2 in Ref. 3).

0.10(1) at every temperature; this average for Ti(2) is 0.08(1) at room temperature and decreases about 30% at 973 K.

To describe more precisely the evolution of the octahedral distortion, Fig. 6 shows the evolution of the short and long Ti-O bonds. For example, in the Ti(2) group [Fig. 6(b)], at 873 K, the shortest Ti(2)-O($t1$) bond starts to increase and the largest Ti(2)-O($t2$) bond decreases to converge towards the same value. Therefore, the lengths of the Ti-O bonds also correlate with the SHG properties. The relationship between these properties and the crystal structure may be established using bond-polarizability theory.[32] Contrary to the study on several isotypes,[11] any other structural parameters cannot be correlated, at least directly, with the SHG efficiency [e.g., Ti(1)-O($t1$)-Ti(2)]. Therefore, before a model is developed to estimate the tensor components of the second-order susceptibility d_{ijk}, they must be measured precisely, i.e., by single crystal methods.[33]

SUMMARY AND CONCLUSIONS

The evolution to centrosymmetry of the RbTP structure was determined by accurate x-ray-diffraction measurements. Excellent agreement was obtained using two refinement models: anharmonicity of Rb and the split atom model. Then it can be directly applied to more complicated studies (i.e., solid solution, $K_{1-x}Rb_xTiOPO_4$).

The evolution of the structure versus temperature is in good agreement with other studies: the evolution of the octahedral distortions (which show the convergence to a local symmetry $\bar{1}^6$) is more important for Ti(2); it corresponds to the partial ordering in the substitution of Ti (Ref. 34) or to the localization of Fe^{3+} impurities.[35] The large displacement of the Rb ions from their room-temperature position[6,12] suggests[31] the second-order phase transition.[3] Contrary to the pressure study on KTP,[12] which shows that the displacement

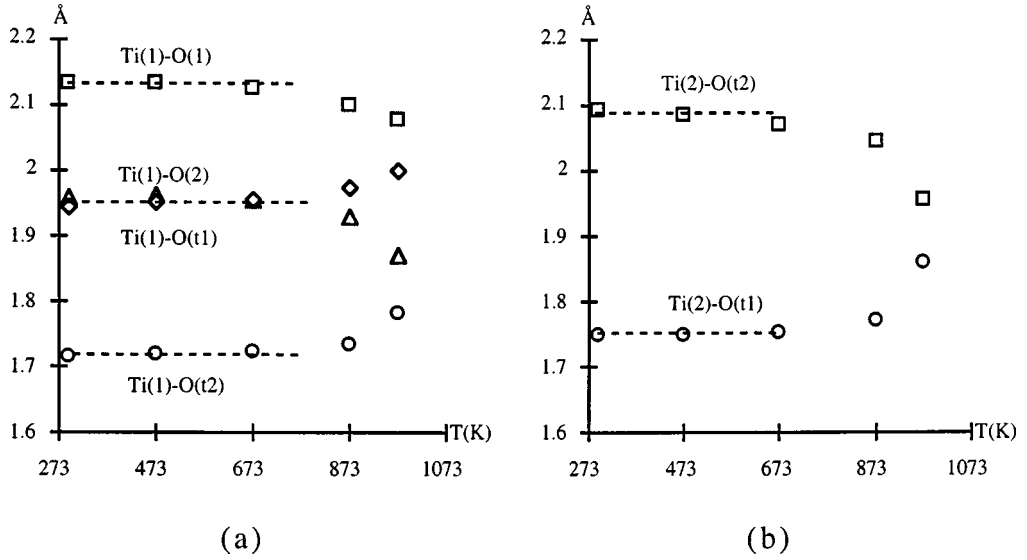

FIG. 6. Evolution of some Ti-O bond lengths (Å) for the Ti(1) site (a) and for the Ti(2) site (b), versus temperature (K).

of the alkaline ions is negligible until the transition and become rapidly maximum at this high-pressure transition, this displacement is gradual versus temperature, and it permits the analysis of its influence on the framework. The splitting of the Rb sites shows that the alkaline ions may be considered as a catalyst of the phase transition. This model describes also the diffusion paths of the high anisotropic ionic conductivity.

If the influence of the alkaline sites is important, the study of the divergence from a centrosymmetric structure shows that the TiO_6/PO_4 framework is directly correlated with the SHG power. Indeed, the evolution of this framework deviation to the centrosymmetry, which is mainly due to the titanyl groups, corresponds exactly to the evolution[13] of SHG intensity $I_{2\omega}$ versus temperature. We have to measure precisely the evolution of the second-order susceptibility tensor components versus temperature to develop a model based on this evolution of these structural parameters.

ACKNOWLEDGMENTS

Dr. Slimane Dahaoui (LCM^3B) is gratefully acknowledged for helpful discussions. The support of University Henri Poincaré, Nancy I, University of Bourgogne and the CNRS is also gratefully acknowledged. P. Delarue is grateful to the Région Lorraine for financial support.

*Author to whom correspondence should be addressed.

[1] R. Masse and J. C. Grenier, Bull. Soc. Fr. Mineral. Cristallogr. **94**, 437 (1971).
[2] I. Tordjman, R. Masse, and J. C. Guitel, Z. Kristallogr. **139**, 103 (1974).
[3] V. K. Yanovskii and V. I. Voronkova, Phys. Status Solidi A **93**, 665 (1986).
[4] D. K. T. Chu, H. Hsiung, L. K. Cheng, and J. D. Bierlein, IEEE Trans. Ultrason. Ferroelectr. Freq. Control **40**, 819 (1993).
[5] J. Y. Wang, Y. G. Liu, J. Q. Wei, L. P. Shi, and M. Wang, Z. Kristallogr. **191**, 231 (1990).
[6] W. T. A. Harrison, T. E. Gier, G. D. Stucky, and A. J. Schultz, Mater. Res. Bull. **30**, 1341 (1995).
[7] F. C. Zumsteg, J. D. Bierlein, and T. E. Gier, J. Appl. Phys. **47**, 4980 (1976).
[8] N. K. Hansen, J. Protas, and G. Marnier, C. R. Acad. Sci., Ser. II: Mec. Phys., Chim., Sci. Terre Univers **307**, 475 (1988).
[9] G. D. Stucky, M. L. F. Phillips, and T. E. Gier, Chem. Mater. **1**, 492 (1989).
[10] P. A. Thomas, A. M. Glazer, and B. E. Watts, Acta Crystallogr., Sect. B: Struct. Sci. **46**, 333 (1990).
[11] M. L. F. Phillips, W. T. A. Harrison, and G. D. Stucky, Proc. SPIE **1561**, 84 (1991).
[12] D. R. Allan and R. J. Nelmes, J. Phys.: Condens. Matter **8**, 2337 (1996).
[13] S. Y. Stefanovich and Y. N. Venevtsev, Izv. Akad. Nauk SSSR, Ser. Fiz. **41**, 537 (1977).
[14] G. Marnier, B. Boulanger, B. Menaert, and M. Metzger, French patent (CNRS) No. 87 00811 (1987).
[15] M. Jannin and P. Delarue (unpublished).
[16] R. Argoud and J. J. Capponi, J. Appl. Crystallogr. **17**, 420 (1984).
[17] R. H. Blessing, Crystallogr. Rev. **1**, 3 (1987).
[18] L. E. McCandlish, G. H. Stout, and L. C. Andrews, Acta Crystallogr., Sect. A: Cryst. Phys., Diffr., Theor. Gen. Crystallogr. **31**, 245 (1975).
[19] G. T. DeTitta, J. Appl. Crystallogr. **18**, 75 (1985).
[20] R. H. Blessing, Acta Crystallogr., Sect. A: Found. Crystallogr. **51**, 33 (1995).
[21] S. Dahaoui, Ph.D. thesis, University Henri Poincaré, Nancy I, 1996.
[22] N. K. Hansen and P. Coppens, Acta Crystallogr., Sect. A: Cryst. Phys., Diffr., Theor. Gen. Crystallogr. **34**, 909 (1978); MOLLY: Aspherical pseudoatom refinement on x-ray diffraction data, N. K. Hansen, LCM^3B, University Henry Poincaré, Nancy I, France.
[23] D. Rez, P. Rez, and I. Grant, Acta Crystallogr., Sect. A: Found. Crystallogr. **50**, 481 (1994).
[24] E. Clementi, IBM J. Res. Dev. **9**, 2 (1965).
[25] E. N. Maslen, A. G. Fox, and M. A. O'Keefe, *International Tables for X-ray Crystallography*, edited by A. J. C. Wilson

(Kluwer, Dordrecht, 1992), Vol. C, p. 219.

[26] J. A. Ibers and W. C. Halmilton, *International Tables for X-ray Crystallography* (Ref. 25), Vol. IV.

[27] See AIP Document No. PAPS: PRBMDO-58-082833 for 10 pages of structure parameters obtained at 293, 473, 673, 873, and 973 K with each model. Order by PAPS number and journal reference from American Institute of Physics, Physics Auxiliary Publication Service, Carolyn Gehlbach, 500 Sunnyside Boulevard, Woodbury, NY 11797-2999. Fax: 516-576-2223, e-mail: paps@aip.org. The price is $1.50 for each microfiche (98 pages) or $5.00 for photocopies of up to 30 pages, and $0.15 for each additional page over 30 pages. Airmail additional. Make checks payable to the American Institute of Physics.

[28] D. K. T. Chu, J. D. Bierlein, and R. G. Hunsperger, IEEE Trans. Ultrason. Ferroelectr. Freq. Control **39**, 683 (1992).

[29] P. A. Thomas and A. M. Glazer, J. Appl. Crystallogr. **24**, 968 (1991).

[30] Y. Le Page, J. Appl. Crystallogr. **21**, 983 (1988).

[31] S. C. Abrahams, Acta Crystallogr., Sect. B: Struct. Sci. **44**, 585 (1988).

[32] B. F. Levine, Phys. Rev. B **10**, 1655 (1974).

[33] B. Boulanger, J. P. Fève, G. Marnier, C. Bonnin, P. Villeval, and J. J. Zondy, J. Opt. Soc. Am. B **14**, 1380 (1997).

[34] S. J. Crennell, J. J. Owen, A. K. Cheetham, J. A. Kaduk, and R. H. Jarman, Eur. J. Solid State Inorg. Chem. **28**, 397 (1991).

[35] J. F. Stenger, Y. Dusausoy, G. Marnier, H. Rager, and J. M. Gaite, J. Phys.: Condens. Matter **1**, 4643 (1989).